First publ. in: Europhysics letters 8 (1989),1, pp. 59-65

Homogeneous Nucleation in Liquid ^{3}He-^{4}He Mixtures.

J. BODENSOHN, S. KLESY and P. LEIDERER
Institut für Physik, Johannes Gutenberg-Universität - Mainz

(received 20 July 1988; accepted in final form 14 October 1988)

PACS. 67.60 – Mixed systems; liquid helium 3-4 mixtures.
PACS. 64.70 – Phase equilibria, phase transitions, and critical points.
PACS. 64.75 – Solubility, segregation, and mixing.

Abstract. – We have investigated the rate of homogeneous nucleation in liquid ^{3}He-^{4}He mixtures as a function of the speed at which the system is quenched into the miscibility gap below the tricritical point. Raising the quench speed $d\tau/dt$ (the derivative of the reduced temperature τ with respect to time) leads to a pronounced increase of the number density N of the droplets which develop during the quench. The data suggest a power law dependence $N \sim (d\tau/dt)^{1.55\pm0.1}$.

The phase separation of binary mixtures is a phenomenon which, due to its importance for material properties and technical applications, has been investigated for many decades [1]. Yet the dynamics of the phase separation process is still incompletely understood [2]. In the past the aim of most experiments was to locate the cloud line, *i.e.* the border of metastability in the miscibility gap of a supersaturated liquid mixture, where nucleation sets in on a laboratory time scale. Experimental information about details of the nucleation process itself, however, is rather sparse. This holds in particular for the dependence of the nucleation rate on the supersaturation of the mixture, which we address in this letter.

One possible method to investigate this problem has been used by Siebert and Knobler [3]: the system is quenched «instantaneously» to a certain point in the miscibility gap, where it is kept for a given amount of time, and the droplets that emerge during that period are counted afterwards. Similar experiments were carried out by Kampmann and Wagner [4], who investigated the early stages of decomposition of solid alloys by small-angle neutron scattering (SANS).

An alternative method, which also appears to be of practical importance, is to vary the speed at which the system is quenched into the miscibility gap, and to measure the density of the nucleating droplets as a function of the quench speed. To our knowledge this technique is applied here to simple liquids for the first time.

Our systems are liquid ^{3}He-^{4}He mixtures, which already have been the subject of nucleation experiments [5, 6]. Below the tricritical point (temperature $T_t = 0.867$ K and ^{3}He concentration $X_t = 0.671$ at saturated vapour pressure) these mixtures exhibit a miscibility gap, which is shifted to lower temperatures as the pressure is raised [7]. This behaviour is

shown in fig. 1, where all the notations used in the text are explained. The dependence of T_t on the pressure enables one to quench the system by decompression, which allows one to reach much higher effective quench speeds than for a temperature quench. Apart from other advantages, the high purity that can be easily achieved in liquid helium suppresses heterogeneous nucleation, an important condition for the unequivocal observation of homogeneous nucleation effects.

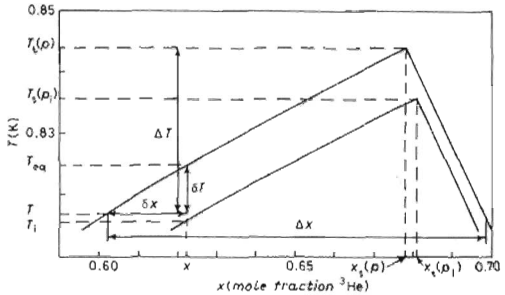

Fig. 1. – Coexistence curve of liquid ^{3}He-^{4}He mixtures for $p_i = 880$ mbar and $p = 570$ mbar. x_i, T_i and p_i are the initial equilibrium values of concentration, temperature and pressure. T is the actual temperature, taking into account the raise of temperature due to the adiabatic decompression.

As mentioned in previous work [5] the cloud line for the ^{3}He-^{4}He system far away from the tricritical point is well described by the classical Becker-Döring theory [1], where the maximum supersaturation depends only on the distance from the tricritical point. For reduced temperatures $\tau = (T_t - T)/T_t$ less than about 0.03, however, the observed maximum supersaturation is more and more enhanced, an effect which is ascribed to critical slowing-down [8, 9]. All the quenches presented in the following started from an equilibrium state at a pressure $p_i \approx 880$ mbar on the superfluid branch of the coexistence curve 17 mK below $T_t(p_i)$, corresponding to $\tau = 0.02$.

Decompression of the mixture was initiated by opening a solenoid valve between the sample cell capillary and a storage tank at room temperature. The quench speed, given by the pressure decay dp/dt in the cell, could be adjusted by changing the initial pressure difference between sample and storage tank, or by reducing the gas flow with an additional valve. The variation of the sample pressure was measured directly in the cell using an interferometric method [10]. Thus, although the pressure drop and hence the quench depth are not varying linearly, but rather exponentially in time, the momentary quench speed could be determined with an accuracy of 10 percent. Typical values of dp/dt ranged from 600 to 9000 mbar/s. Using the known pressure dependence of the tricritical point, this can also be expressed in terms of a quench in reduced temperature units and amounts to $d\tau/dt$ between $2 \cdot 10^{-2}$ s and $3 \cdot 10^{-1}$ s. For calculating the supercooling one has to take into account the slight temperature change due to the adiabatic decompression, which in the case of liquid ^{3}He-^{4}He raises the temperature. The total time for a quench was typically on the order of one second.

The decomposition process was monitored by measuring the optical transmissivity of the sample using a focussed low-power laser beam (10^{-5} W). Some results are shown in fig. 2, where the transmitted intensity, normalized with respect to the intensity I_0, is plotted *vs.* a

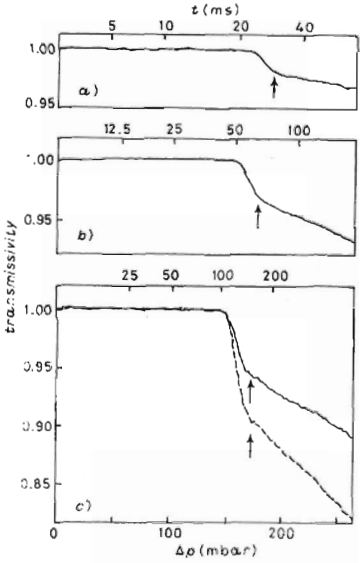

Fig. 2. – Intensity of a He-Ne laser beam ($\lambda = 633$ nm) after transmission through a ^{3}He-^{4}He sample undergoing phase separation, normalized to the incident intensity I_0. The quench speeds are *a*) 7000 mbar/s, *b*) 1300 mbar/s, *c*) 600 mbar/s at the onset of nucleation. The dashed line in *c*) represents the transmissivity at a second light wavelength ($\lambda = 488$ nm). The sudden drop in intensity around $\Delta p \approx 150$ mbar is due to the nucleation of droplets at the «cloud point». The arrows mark the beginning of the range where local decomposition is essentially completed and the droplet number is evaluated (see fig. 3).

linear scale of the quench depth $\Delta p = p_c - p(t)$ for three different quench speeds. The values for dp/dt, evaluated at the onset of nucleation, were 600, 1300, and 7000 mbar/s, respectively. Note that the time scales in this figure are nonlinear. As the cloud point is reached, the transmissivity drops due to light scattered out of the primary beam by the nucleating droplets.

Several stages can be distinguished:

the metastable state, where the system is stable on the given time scale, and hence the laser beam is not attenuated;

nucleation and subsequent local decomposition by growth of the droplets, which is a rapid process and gives rise to the steep decrease in the intensity;

further slow growth of the droplets formed in the second stage, because the pressure continues to drop and the system «slides down» along the coexistence curve.

The observed behaviour is in agreement with that found by others [5, 6]. The final stages of decomposition, namely droplet growth by coagulation and gravitationally induced growth, are slow and, therefore, do not contribute on the time scale shown here. The step

signalling the cloud point occurs at nearly the same pressure Δp_c for the various traces in fig. 2. The maximum supercooling $\delta T/\Delta T = (T_{eq} - T)/(T_\lambda - T)$ calculated from Δp_c changes slightly from 0.25 to 0.28 as the quench speed is increased by one order of magnitude, in qualitative agreement with ref. [6]. (Here T_{eq} is the equilibrium temperature on the coexistence curve for the initial concentration; see fig. 1.) This dependence and the absolute values of $\delta T/\Delta T$ reflect the influence of critical slowing-down. (The classical Becker-Döring theory yields a constant value $\delta T/\Delta T \approx 0.13$.)

In contrast to the position of the step which shifts only by about ten percent, the *height* of the steps changes quite markedly with dp/dt. The data imply that the density of the nucleating droplets increases strongly as the quench speed is raised. This is shown by the following analysis of the transmitted light intensity I, which is given by the extinction formula

$$I = I_0 \cdot \exp\{-N \cdot C_{tot} \cdot l\}. \tag{1}$$

Here I_0 is the intensity of the incident light, N is the number density of droplets, l is the length of the scattering volume and C_{tot} is the total scattering cross-section of one droplet, in our approach considered as a nonabsorbing sphere of radius a. As long as the radius is small compared to the light wavelength λ, one has simple Rayleigh scattering where the dependence of the cross-section on the wave vector $k = 2\pi/\lambda$ and the droplet radius is given by $C_{tot} \sim k^4 a^6$. Scattering becomes more complicated if the radius is comparable to the light wavelength. If the difference of the refractive indices n_1 and n_2 of the inside and the outside of the sphere is small, however, so that the condition $2|(n_1/n_2) - 1|ka \ll 1$ holds (as is the case for the helium mixtures), the total cross-section should obey the Rayleigh-Gans formula [11]

$$C_{tot} = 2\pi(n_1/n_2 - 1)^2 k^2 a^4. \tag{2}$$

In order to test whether the Rayleigh or the Rayleigh-Gans limit apply in our case we have measured the transmissivity I/I_0 of the sample simultaneously at two different wave vectors. For this purpose two collinear laser beams with wavelengths $\lambda_1 = 633$ nm and $\lambda_2 = 488$ nm probed the same region of the sample, and, after having passed the cell, were registered separately. We found that in the regime experimentally accessible to us (extinction > 0.005) the wave vector dependence was very well described by eq. (2). Therefore, we have used the Rayleigh-Gans approximation for the further analysis. From the transmissivity data in fig. 2 the number density N of the droplets can, therefore, be calculated using eqs. (1) and (2) together with the fact that the volume fraction of the minority phase, which is given by the relative supersaturation $\delta x/\Delta x$ is equal to $(4\pi/3)\ Na^3$. It should be pointed out that multiple scattering, which in general severely hampers decomposition studies by light, is negligible here even for our large sample thickness of 1 cm because of the small difference between the refractive indices of the superfluid (^{4}He-rich) and the normal (^{3}He-rich) phase.

The resulting densities are plotted in fig. 3. Two simplifications have been made here: i) instead of integrating over a distribution of droplet sizes we have used an effective average droplet radius a; ii) since for the present purpose only data close to the completion of the local decomposition are considered, we have taken for the concentrations the values on the coexistence curve. The error introduced by the second approximation has been estimated by a calculation of the stable droplet size according to Lifshitz and Slyozov [12], which yields the momentary concentrations of the droplets and the background phase. From this model calculation we conclude that the actual concentrations deviate only by 10^{-4} from the equilibrium values given by the coexistence curve. As to the finite width Δa of the droplet

distribution function, an estimate for its influence on the signal was obtained by calculating the extinction for several distributions of droplet radii. It was found that this gives rise to only a slight shift of the calculated value of a, provided the distribution is relatively narrow ($\Delta a < a$) as is known from other systems [13]. For the following both corrections mentioned above are not relevant, because they are nearly the same for the various quench speeds and, therefore, drop out as long as only relative changes are considered.

As the curves in fig. 3 indicate, the droplet density remains essentially constant for $\Delta p > 200$ mbar. At first glance this might be in contradiction with the data in fig. 2, where the transmitted intensity continuously decreases in this range. However, this drop in intensity is primarily due to a growth of the average droplet radius as the system is drifting away from the tricritical point, and the volume fraction of the minority phase, therefore, increases. It is obvious that in the depicted range the process of coagulation, which eventually leads to a decrease of the number of droplets, has not noticeably set in yet. Thus the droplet density near completion of the local decomposition is a well-defined quantity in this experiment. According to fig. 3 the droplet density grows by a factor of 40 as the quench

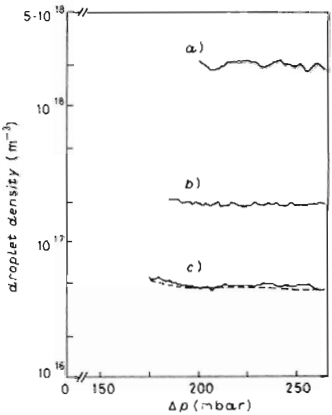

Fig. 3.

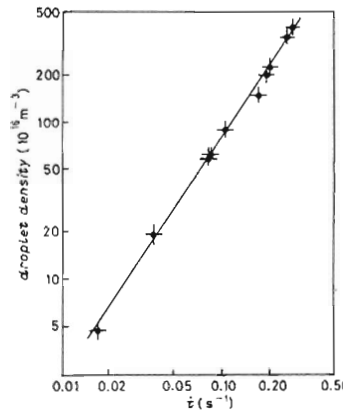

Fig. 4.

Fig. 3. – Number density N of droplets *vs.* quench depth Δp, calculated from eq. (3) for the three quenches shown in fig. 2. For *c*) the solid line refers to a light wavelength $\lambda = 633$ nm and the dashed line to $\lambda = 488$ nm. Note that the calculation for the two light wavelengths in *c*) yields the same droplet densities, confirming the validity of the Rayleigh-Gans approximation. The corresponding droplet sizes at the beginning and the end of each representation are *a*) $2.2 \cdot 10^{-7}$ m, $2.8 \cdot 10^{-7}$ m; *b*) $5.3 \cdot 10^{-7}$ m, $6.1 \cdot 10^{-7}$ m; *c*) $8.1 \cdot 10^{-7}$ m, $10.1 \cdot 10^{-7}$ m.

Fig. 4. – Number density N of the droplets after completion of local decomposition, plotted *vs.* the reduced quench rate $\dot{\tau} = \mathrm{d}\tau/\mathrm{d}t$ at the onset of nucleation. The straight line represents a power law dependence $N \sim (\dot{\tau})^{1.55}$.

speed is raised from 600 to 7000 mbar/s. More explicitly, the dependence between N and $\mathrm{d}\tau/\mathrm{d}t$ is shown in fig. 4, where in addition data from several other quenches are plotted. The straight line suggests that the data can be represented by a power law $N \sim (\mathrm{d}\tau/\mathrm{d}t)^{1.55 \pm 0.1}$.

A detailed theory for the droplet density developing during a continuous quench is presently not at hand (1). Qualitatively, however, the observed increase of N with growing quench speed can be understood on the basis of a simple argument.

According to Langer and Schwartz [9] one expects that for shallow quenches—small supersaturation—decomposition happens as the result of two competing effects, nucleation and growth of already existing droplets. Consider now an individual ^{3}He-rich droplet in the supersaturated ^{4}He-rich background pahse. As the droplet grows, the ^{4}He concentration in the surrounding phase will be reduced, giving rise to a diffuse «halo» around the droplet with a smaller supersaturation and hence a reduced probability for the nucleation of further droplets in this region. Since the ^{3}He transport is governed by diffusion, the diameter d_H of this halo will vary as $t^{1/2}$, where t is the time after the formation of the droplet. If we for simplicity assume that outside the halo nucleation occurs at a rate determined by the original homogeneous supersaturation, and in the halo nucleation has dropped to zero, then the formation of new droplets will cease when neighbouring halos start to overlap. We compare now two quenches at different speed $\mathrm{d}\tau/\mathrm{d}t$ under otherwise identical conditions. Then the characteristic time where the diffusion process can take place will be inversely proportional to $\mathrm{d}\tau/\mathrm{d}t$, yielding smaller halos the faster the quench. Since at the end of the nucleation stage the average halo diameter should be roughly equal to the average distance of the droplets, *i.e.* $d_H \approx N^{-1/3}$, and, on the other hand, $d_H \sim t^{1/2} \sim (\mathrm{d}\tau/\mathrm{d}t)^{-1/2}$, one expects $N \sim (\mathrm{d}\tau/\mathrm{d}t)^{3/2}$, which is surprisingly close to the experimental value.

We have also tried a more quantitative treatment by simulating the continuous quench by a sequence of stepwise quenches, calculating after each time step the number of critical droplets formed at the given level of (average) supersaturation and growth of the already existing droplets. We have used a nucleation rate published by Langer and Schwartz [9] and calculated the droplet growth according to the Lifshitz-Slyozov growth law [12]. The relation $N \sim (\mathrm{d}\tau/\mathrm{d}t)^y$ with $y \approx 1.5$ and also the absolute densities of the droplets could be reproduced within ten percent. These results will be presented in a separate paper.

In summary, our measurements have established a relationship between the number of droplets evolving during a homogeneous nucleation process, and the speed at which the quench into the miscibility gap occurs. The observation that a faster quench yields a larger droplet density might have been expected intuitively, because for a faster quench droplets do not have as much time to ripen, and hence the system will be forced somewhat deeper into the unstable regime, with a correspondingly larger nucleation rate. We hope that the data presented here will stimulate the theoretical treatment of the nucleation process under the conditions of a continuous quench, which for a number of practical purposes appears to be a more realistic approach than the usual assumption of an instantaneous quench.

* * *

We gratefully acknowledge helpful discussions with K. BINDER and R. FEILE. A system of light guides, which enabled us to use various external laser sources, was kindly supplied by Schott Glaswerke, Mainz.

---

(1) Continuous quenches have already been considered by Rabin, Gitterman and Edrei [14]. These authors concentrate on the early stages of nucleation when the nucleation rate approaches a steady-state value. In contrast, we investigate the total number of droplets formed at the very end of the nucleation process, where the nucleation rate has dropped to zero.

REFERENCES

[1] See, *e.g.*, ABRAHAM F. F., *Homogeneous Nucleation Theory* (Academic Press, New York, N. Y.) 1974; ZETTLEMOYER A. C. (Editor), *Nucleation* (Dekker, New York, N. Y.) 1969.

[2] BINDER K., *Rep. Prog. Phys.*, 50 (1987) 783.

[3] SIEBERT E. D. and KNOBLER C. M., *Phys. Rev. Lett.*, 52 (1984) 1133.

[4] KAMPMANN R. and WAGNER R., *Atomic Transports and Defects in Metals by Neutron Scattering*, edited by C. JANOT, W. PETRY, D. RICHTER and T. SPRINGER (Springer, Berlin) 1986, p. 71.

[5] ALPERN P., BENDA T. and LEIDERER P., *Phys. Rev. Lett.*, 49 (1982) 1267.

[6] SINHA D. N. and HOFFER J. K., *Phys. Rev. Lett.*, 50 (1983) 515; HOFFER J. K. and SINHA D. N., *Phys. Rev. A*, 33 (1986) 1918.

[7] DEL CUETO J. *et al.*, *J. Phys. C*, 41 (1980) 133. Since there are no experimental data about the shift of the tricritical temperature with pressure in the range from s.v.p. up to 1000 mbar, we investigated the shift of T_t in that pressure range and found a dependence similar to that obtained by an interpolation of the data presented in the work cited above.

[8] BINDER K. and STAUFFER D., *Adv. Phys.*, 25 (1976) 343.

[9] LANGER J. S. and SCHWARTZ A. J., *Phys. Rev. A*, 21 (1980) 948.

[10] LEIDERER P. and BOSCH W., *Phys. Rev. Lett.*, 45 (1980) 727.

[11] VAN DER HULST, *Light Scattering by Small Particles* (John Wiley and Sons, New York, N. Y.) 1957.

[12] LIFSHITZ I. and SLYOZOV V., *J. Phys. Chem. Solids*, 19 (1961) 35.

[13] KRISHNAMURTHY S. and GOLDBURG W. I., *Phys. Rev. A*, 22 (1980) 2147.

[14] RABIN Y. and GITTERMAN M., *Phys. Rev. A*, 29 (1984) 1496; EDREI I. and GITTERMAN M., *Phys. Rev. A*, 33 (1986) 2821.